THE JOURNAL OF PHYSICAL CHEMISTRY B

ARTICLE

pubs.acs.org/JPCB

High-Pressure Reactivity of L,L-Lactide

Matteo Ceppatelli,*[,†,‡] Marco Frediani,[‡] and Roberto Bini[†,‡]

[†]LENS, European Laboratory for Nonlinear Spectroscopy, Via Nello Carrara 1, 50019 Sesto Fiorentino (FI), Italy

[‡]Dipartimento di Chimica "Ugo Schiff" dell'Università degli Studi di Firenze, Via della Lastruccia 3, 50019 Sesto Fiorentino (FI), Italy

ABSTRACT: L,L-Lactide, a dimer of L-lactic acid, is the typical monomer used for the catalytic synthesis of poly(L-lactic acid) (PLLA). We studied its phase diagram and reactivity at high pressure and high temperature by means of a diamond anvil cell. FTIR and Raman spectroscopy were employed to probe the changes occurring in the sample. An increase of temperature at pressure higher than 0.1 GPa revealed a solid−solid phase transition before the melting. A reaction was observed immediately after the melting with the almost complete transformation of the starting reactant to an amorphous poly(lactic acid) (PLA). The increase of pressure was found to accelerate the process, suggesting the reaction rate to be limited in the diffusion step. A steeper acceleration, likely due to multiphoton absorption processes of the 647.1 nm laser light by PLA, was observed in the Raman experiments.

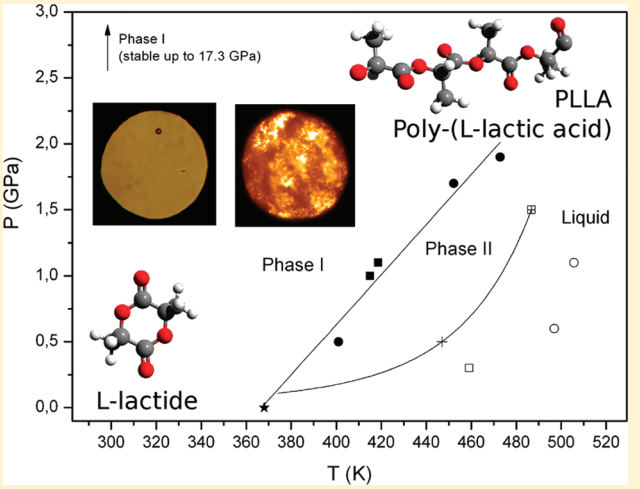

INTRODUCTION

Poly(L-lactic acid) (PLLA) is a renewable and biodegradable polymeric material proving to be a viable alternative to petrochemical-based plastics.[1−3] The basic constitutional unit of PLLA is L-lactic acid, which is generally manufactured by fermentation of carbohydrates or chemical synthesis.[4] The polymer is a nonvolatile odorless material and is classified as GRAS (Generally Recognized As Safe) by the Food and Drug Administration.[5] Recently, to avoid possible competition with the food supply, also the direct production from biomass has started to increase.[6] Nowadays, a wide range of PLLA products can be synthesized that vary in molecular weight, stereochemistry, and crystallinity, allowing this material to have unique physical properties suitable for a variety of applications (medical field, paper coating, fibers, films, packaging, etc.).[7,8] Among the synthetic methods reported in the literature, the ring-opening polymerization (ROP) of L-lactide (the cyclic dimer of L-lactic acid) represents an eligible choice for the synthesis of PLLA polymers with high control on molecular weight and low racemization level[9] (Figure 1). Many catalysts are employed for this kind of polymerization (complexes of aluminum, zinc, tin, lanthanides, metal alkoxides, etc.).[10] Tin compounds, especially tin(II) bis-2-ethylhexanoic acid tin (octanoate), are generally preferred for the bulk polymerization of lactide due to their solubility in molten lactide, high catalytic activity, and low rate of racemization of the polymer.[2,9,10] However, due to the potential toxicity of organotin compounds, the development of new systems containing nontoxic oxophilic metal centers and easy to be synthesized is always attracting more attention.[11]

L-Lactide is a crystalline solid at ambient conditions. The molecule has two stereocenters and can exist as two enantiomers (L,L and D,D, mp 97−98 °C), as the racemic mixture (L,L,D,D mp 125−127 °C), and as the two meso forms (mp 52 °C).[3,12] In this paper, we adopted the literature notation according to which L,L-lactide is shortened to L-lactide. We generically refer to poly(lactic acid) (PLA) when no specification about the stereochemistry is provided. In our experiments, we used the L-lactide isomer, so that in absence of racemization processes the stereochemistry of the monomeirc unit is conserved during the ROP and the expected polymer is PLLA (Figure 1). The interest in the L,L versus the D,D isomer is related to the need of obtaining a bioresorbable and biocompatible material which can be metabolized by mammals. Only the L,L isomer indeed matches these requirements.[8]

The application of moderate pressure in the MPa range is a well established and very effective tool for increasing the yield and selectivity of many chemical processes. Higher pressure, in the GPa range, is more difficult to generate and its use is not so common in chemistry. Nevertheless, many studies have demonstrated that the dramatic increase of density occurring at such high pressure has an extraordinary potential for activating chemical reactions in the condensed phases of molecular systems otherwise stable at ambient conditions.[13] A wealth of new materials of fundamental and applicative interest has been

Received: November 18, 2010
Revised: January 20, 2011
Published: February 18, 2011

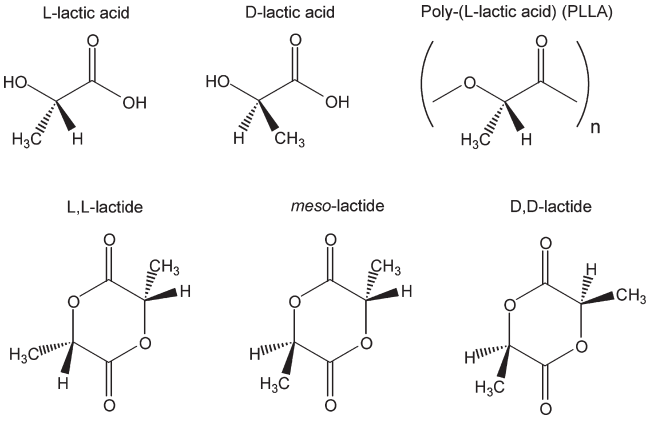

Figure 1. Structural formulas of PLLA and of lactic acid and lactide stereoisomers.

synthesized. Whereas some of them only exist under extreme conditions and their formation is reversible,[14−17] in other cases a reaction product can be recovered at ambient conditions.[18−23] Polymers and amorphous and energetic materials of technological interest have been obtained.[24,25] A comprehensive review about this topic can be found in ref 13. Despite the extreme conditions required by several systems, in some cases the combination of high pressure and photoexcitation has been shown to be very effective in triggering quantitative and selective chemical reactions and lowering the threshold pressure for the reaction.[26] The application of thermodynamic conditions accessible to the actual industrial technologies and the absence of solvent, catalysts, and radical initiators make these processes appealing for possible scaling of the experimental system to large volume apparatuses.[27,28]

Within this context, our study was aimed at the investigation of the high-pressure behavior of L-lactide, focusing to the individuation of the pressure and temperature conditions for the synthesis without catalysts of PLLA.

EXPERIMENTS

L-Lactide was obtained from Aldrich and sublimated before use. High pressure was generated by means of a membrane diamond anvil cell (MDAC) equipped with IIa 600 μm culet tip anvils. The sample was contained sideways by a stainless steel gasket indented to a 50 μm thickness. A 300 μm hole was drilled in the indented region of the gasket by the spark-erosion technique. The hole was filled with 10−30 μm sized particles of gold, and then the gasket was compressed and drilled again to obtain a final hole with a 150 μm diameter. This procedure ensured the gilding of the hole to prevent any catalytic effect due to the stainless steel gasket. A ruby chip was inserted in the sample for the in situ pressure measurements by the R_1 ruby fluorescence band shift method.[29] The ruby fluorescence was excited using few milliwatts of a 532 nm laser line from a duplicated CW Nd:YAG laser source. The high temperature was generated by a resistive heater and was measured by means of a thermocouple placed at less than 1 mm from the sample. The FTIR spectra were recorded with a resolution of 1 cm^{-1}, using a Bruker IFS 120 HR spectrometer equipped with a beam condensing optical bench and modified to host a MDAC, allowing FTIR high-pressure experiments in the 15−800 K range.[30,31] The Raman spectra were recorded using the 647.1 nm line of a Kr ion laser source with laser power ranging from 40 to 115 mW.

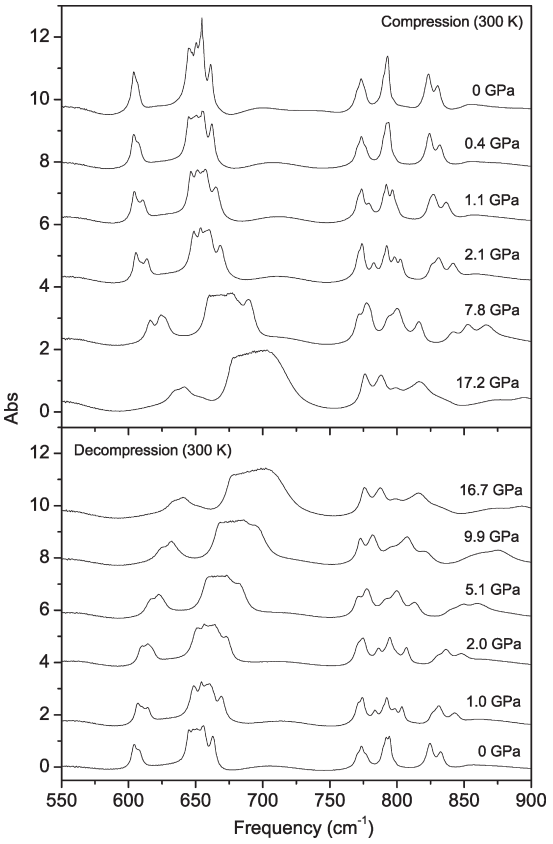

Figure 2. Selected region of the FTIR spectra recorded during the compression (upper panel) and decompression (lower panel) at 300 K. The spectra at 0 GPa before and after the compression−decompression cycle are nearly identical, indicating the stability of L-lactide at 300 K in the investigated pressure range.

The Raman signal was collected in a back scattering configuration, filtered through a spatial filter, diffracted by a monochromator (Acton TR555), and recorded on a liquid nitrogen cooled CCD detector. The stray light was filtered out through two notch filters. The monochromator was used in the single-stage configuration with a 900 grooves/mm grating and a 50 μm entrance slit to optimize resolution (~0.7 cm^{-1}) and acquisition time.

RESULTS

Several FTIR and Raman experiments in different pressure and temperature conditions were performed. For the sake of clarity, they are reported in two separate subsections.

FTIR Spectra. The high-pressure stability of L-lactide was probed at room temperature by FTIR spectroscopy along an isothermal compression−decompression cycle up to 17.3 GPa. The pressure was increased in steps of 0.5 GPa, waiting 1 h after each pressure increase. A slight asymmetry was detected in several bands at ambient pressure, but their clear splitting was observed during the compression between 0.4 and 1.0 GPa. This splitting is shown in Figure 2 for a selected region of the infrared spectrum, but a similar behavior was observed in all the investigated frequency range between 500 and 5000 cm^{-1}. Besides the typical pressure shift and line broadening, no spectral changes that could be related to the occurrence of a chemical reaction were detected. With the exception of some minor intensity changes in a few bands, the spectra recorded before and after the

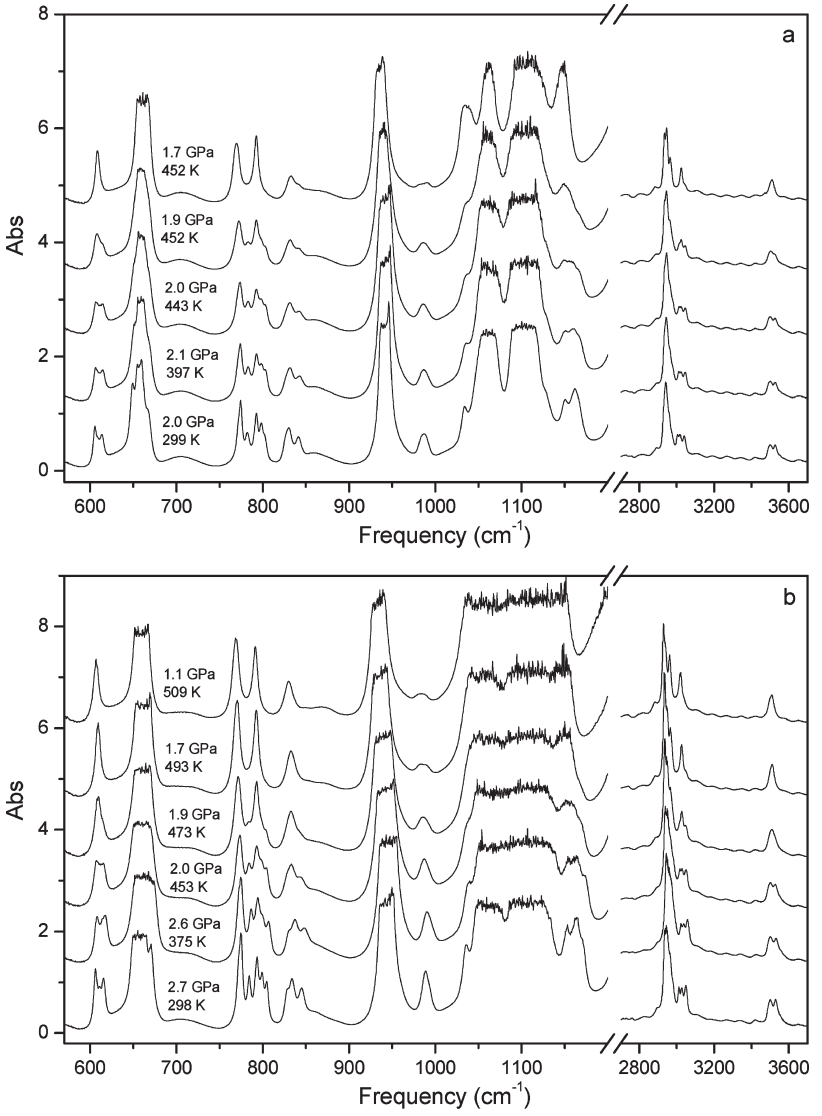

Figure 3. Evolution of the FTIR spectra in the 550−1500 cm^{-1} and in the 2700−3700 cm^{-1} frequency ranges during two different experiments. Upper panel (a): isobaric heating at about 2.0 GPa. Lower panel (b): heating with continuous pressure reduction.

compression−decompression cycle were identical, thus indicating the stability of L-lactide at room temperature up to the maximum pressure reached. Several heating cycles at different pressures were performed for testing the L-lactide stability with increasing temperature. On the basis of the results from the room temperature compression−decompression cycle, in all these experiments we first compressed the sample at 300 K up to the desired pressure and then started to heat. During the heating we observed some spectral changes and then, for a higher temperature, the occurrence of a chemical reaction, revealed by the intensity decrease of the L-lactide bands and by the appearance of new absorptions. The spectral changes occurring before the reaction are reported in Figure 3 for two different experiments. The splitting of all the bands abruptly disappeared between 450 and 470 K and 1.8 (±0.1) GPa, suggesting a structural change of the L-lactide crystal. This behavior was also evident in the C−H stretching region. Once the sample was brought back to ambient conditions, we could not recover the FTIR spectrum of L-lactide as loaded. The FTIR spectrum was indeed similar to that of L-lactide at high pressure and high temperature (Figure 4).

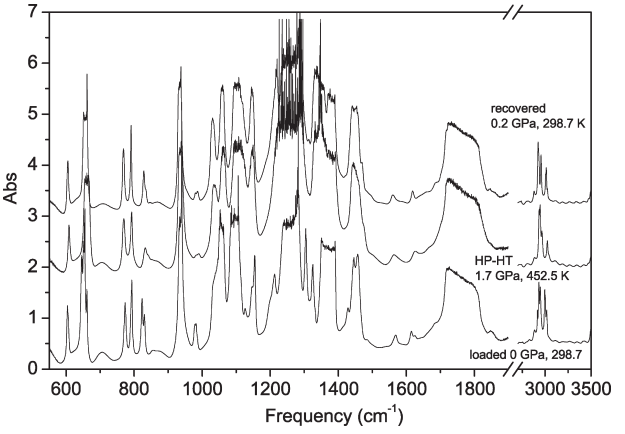

Figure 4. Comparison between the FTIR spectra recorded after the loading (lower trace), at the highest pressure (HP) and temperature (HT) conditions (middle trace) and after (upper trace) a compression−heating−cooling−decompression cycle within the stability region for the molecular crystal.

dx.doi.org/10.1021/jp1110136 |J. Phys. Chem. B 2011, 115, 2173–2184

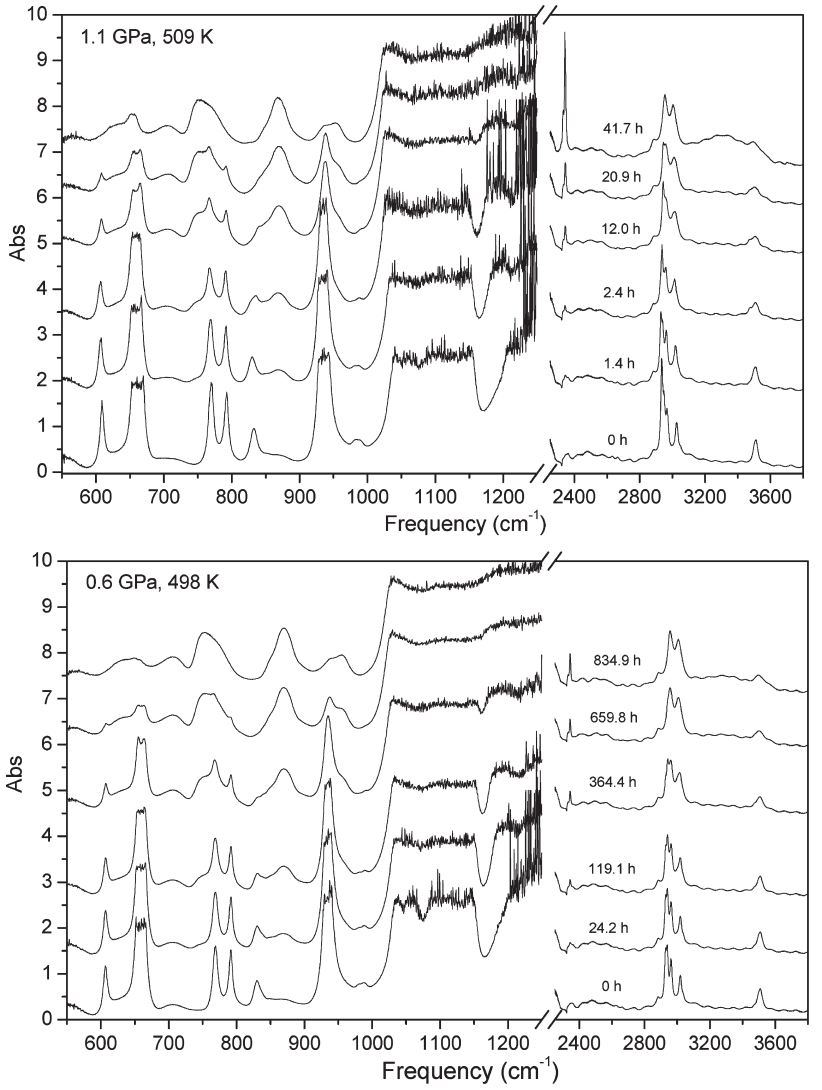

Figure 5. Time evolution of the FTIR spectra during the reactions at 1.1 GPa and 509 K (upper panel) and at 0.6 GPa and 498 K (lower panel).

The reaction evolution was followed at 0.6 GPa and 498 K and at 1.1 GPa and 509 K at constant thermodynamic conditions. The reaction was first revealed by the appearance of broad absorptions peaked at 746, 870, and 956 cm^{-1} and by the weakening of the L-lactide bands. The time evolutions of the spectra in the two different sets of conditions are reported in Figure 5. As the reaction proceeded, the bands of L-lactide progressively weakened and were not observable anymore at the end of the reaction, indicating the complete transformation of the reactant. A sharp band at 2343 cm^{-1} and a weak and broad absorption encompassing the frequency range between 3200 and 3600 cm^{-1} also appeared during the reaction. Whereas the first one, assigned to the antisymmetric stretching (ν_2) of CO_2, was already observable in the early stages of the reaction, the second one, likely due to O−H stretching modes, became evident only when almost all the L-lactide was consumed. The growth of the second absorption coincided with a steep increase in the rate of formation of the first band, thus suggesting the opening of a decomposition channel for the reaction product. The CO_2 bending (ν_3) absorption was hidden by the L-lactide absorption at 656 cm^{-1}, but its presence became evident when recovering the ambient conditions (Figure 6).

A significant issue to be pointed out is related to the very different time scale on which the reaction occurred in the two experiments. At 1.1 GPa and 509 K the reaction was completed within 42 h, but at 0.6 GPa and 498 K more than 835 h were necessary to transform all the L-lactide. In this latter case, we continuously monitored the growth of the CO_2 absorption at 2343 cm^{-1}. This procedure allowed us to detect any sudden increase in the rate of CO_2 formation. Using this method, we were able to immediately stop the reaction by quickly cooling the sample, thus avoiding an extensive decomposition of the reaction product.

On cooling the sample and releasing the pressure, in spite of the band narrowing, no big changes were observed in the spectrum (see the spectra in Figure 6). The major change was related to the disappearance of the CO_2 bands after the opening of the cell. The recovered solid sample from the reaction at 1.1 GPa and 509 K was photographed at room temperature by means of a microscope (Figure 6). As long as some residual pressure was applied, the sample looked transparent like at high temperature (Figure 6, photo b). Nevertheless, after the residual pressure was removed, the sample showed an opaque granular structure which could be appreciated with both transmitted

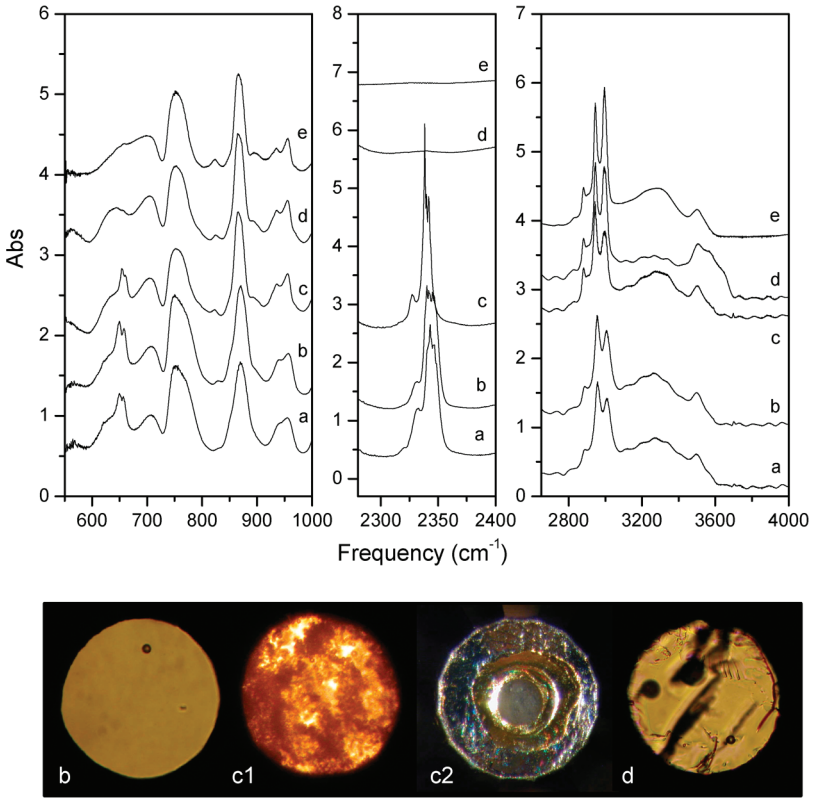

Figure 6. Selected regions of the FTIR spectra measured during the cooling and decompression after the reaction at 1.1 GPa and 509 K. The labels in the spectra refer to the following conditions: (a) 1.4 GPa, 452 K; (b) 1.0 GPa, 306 K (photo b); (c) 0 GPa, 299 K (the membrane pressure was released, but the cell was still closed, as evidenced by the presence of the CO_2 bands; photo c1 in transmission and c2 in reflection); (d) 0 GPa, 298 K (after opening and reclosing the cell; photo d in transmission); and (e) 0 GPa, 298 K (recovered sample outside the cell). The disappearance of the CO_2 after the cell is opened is clearly evident at ~650 cm^{-1} and in the 2300−2400 cm^{-1} frequency range, where the bending and the antisymmetric stretching, respectively, disappear.

(Figure 6, photo c1) and reflected light (Figure 6, photo c2). After the cell was opened, the granular structure was lost and the sample appeared more transparent (Figure 6, photo d).

Raman Spectra. Raman experiments were performed on increasing temperature along nonisobaric paths until the melting. The reaction was followed at 0.3 GPa and 459 K and at 1.5 GPa and 487 K (Figure 7). On increasing the temperature, several characteristic spectral changes, likely indicating a structural change of the L-lactide crystal, were observed. As already observed in the FTIR spectra, the splitting of several doublets (449, 481, 605, 660, 792 cm^{-1}) was removed at ~400 K. In addition, significant changes were observed in the phonon frequency range, where the structured profile due to the lattice modes markedly transformed into three sharp bands at 48, 65, and 83 cm^{-1}. With a further increase in temperature (~450 K at 0.5 GPa and ~490 K at 1.0 GPa), the structured profile of the lattice phonons faded into a characteristic broad band typical of liquid systems, thus suggesting the L-lactide melting. This hypothesis was also supported by the real time visual observation of the sample, by means of a camera coupled to the Raman system, that revealed a displacement of the ruby chip. In the higher pressure experiment, as the melting occurred, all the Raman bands of L-lactide decreased in intensity, whereas a new strong band started to be observed at 873 cm^{-1}, indicating the occurrence of a chemical transformation of L-lactide. In the lower pressure experiment, the appearance of the new bands occurred at higher temperature with respect to the melting. Comparing the Raman experiment at 1.5 GPa with the FTIR experiment at 1.1 GPa and the Raman experiment at 0.3 GPa with the FTIR experiment at 0.6 GPa, the time scale for the reactive processes in the Raman experiments (~3 h in both cases) was shorter by a factor 14 and 278, respectively. The much faster reaction rate observed in the Raman experiments suggests the involvement in the reactive process of the laser light used to measure the spectra.

No special ramp was adopted for cooling the sample to ambient temperature. The spectra recorded during the cooling showed an overwhelming fluorescence background, which prevented any detection of the Raman signal from the reaction product. Furthermore, in this case the laser spot used to perform the Raman experiment seemed to damage the sample (see the black spot visible in Figure 8, photos a−c). The photographs of the recovered sample from the Raman experiment at 0.3 GPa and 450 K showed a material characterized by a homogeneous bubble distribution (Figure 8, photos a and b). The imprint shape of the bubbles was still visible in the recovered sample after the opening of the cell (Figure 8, photo c). The FTIR spectrum of the recovered sample was completely different from that measured before the Raman experiment, indicating the transformation of L-lactide to a different reaction product (Figure 8). The release of pressure at ambient temperature did not induce any change in the IR spectrum. Nevertheless, after the opening of the cell, the CO_2 bands at 660 and 2341 cm^{-1} were not present any more in the spectrum, indicating that CO_2 left the sample after the opening of the cell. A slight modification of the absorption

dx.doi.org/10.1021/jp1110136 |J. Phys. Chem. B 2011, 115, 2173–2184

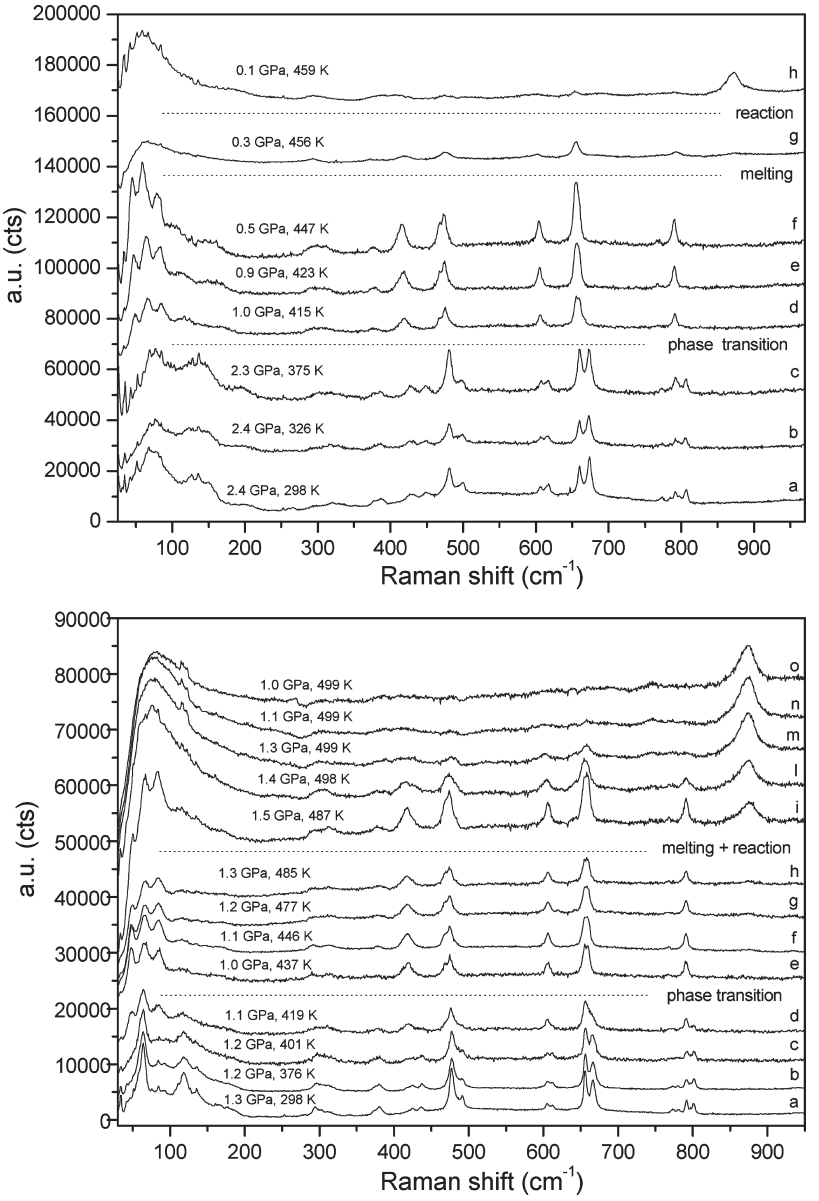

Figure 7. Evolution of the Raman spectra in a selected frequency region during the phase transition, the melting, and the reaction of L-lactide in two different experiments at 0.3 GPa, 459 K (upper panel) and 1.5 GPa, 487 K (lower panel). The labels on the right-hand side are just a reference for the reader.

profile was revealed in the 2800−3600 cm^{-1} frequency range. An analogous behavior was observed in the case of the reaction occurred at 1.5 GPa and 487 K.

In all the FTIR and Raman experiments, the reaction product recovered at ambient conditions appeared as a transparent gel-like material, which became completely transparent by a slight hand compression of the diamond anvils.

Phase Diagram. With the exception of the melting point at room pressure, to our knowledge no literature data about the phase diagram of L-lactide are available. The first goal of this study was then to trace a phase diagram of L-lactide, in order to individuate the melting line and identify the stability range of the molecule. The crystal structure of the L,L and D,D racemate has been studied at ambient conditions by X-ray diffraction (XRD).[32] The space group is $P2_1/c$ with $Z = 4$ and the molecule has C_2 symmetry. FTIR measurements showed the L-lactide crystal to be stable at room temperature at least up to 17.3 GPa. During the room temperature compression several bands in the internal modes region, all of them showing clear asymmetries also at low pressure, exhibited a progressive splitting, spread over several GPa. The structured profile of the lattice phonons was not altered by pressure, thus suggesting that the band splitting of the internal modes was likely due to an increased frequency separation of the Davydov components with pressure rather than to a phase transition to a different crystal structure. A splitting of every vibrational mode into two components is indeed expected according to the structure proposed for the L,L and D,D racemate crystal.[32]

The Raman spectra measured during the heating of L-lactide along the isobar at 0.1 GPa, both in the external and in the internal mode region, did not indicate the presence of any phase transition from the crystal phase stable at ambient conditions, which we will refer to as phase I, until the melting.

dx.doi.org/10.1021/jp1110136 |J. Phys. Chem. B 2011, 115, 2173–2184

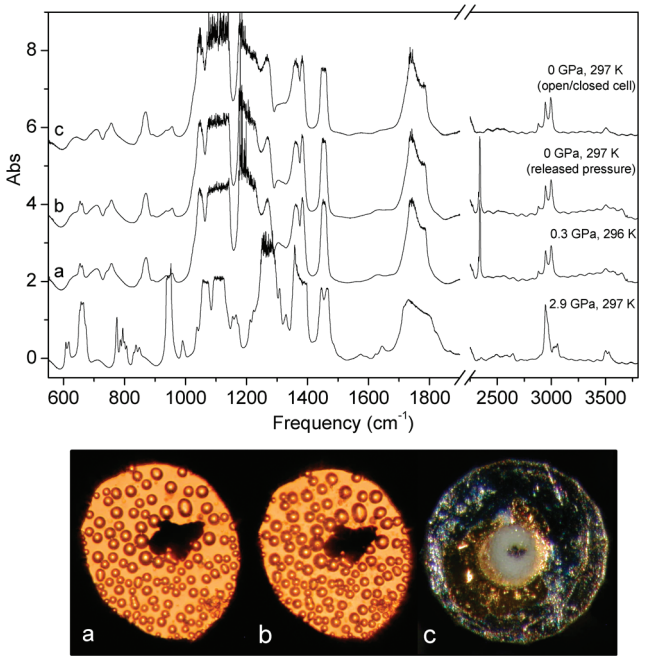

Figure 8. FTIR spectra of the sample recovered from the reaction occurring at 0.3 GPa and 459 K (followed by Raman spectroscopy). The bottom spectrum refers to the room temperature pressurized sample after the loading. The microphotographs (a and b in transmission, c in reflection) refer to the spectra with the corresponding labels. The presence of bubbles is in agreement with the observation of CO_2 in the FTIR spectra. The dark spot in the center of the sample is the trace left by the laser after the reaction (see text for details). Also in this case the disappearance of the CO_2 bands after the cell was opened is evident from the spectra.

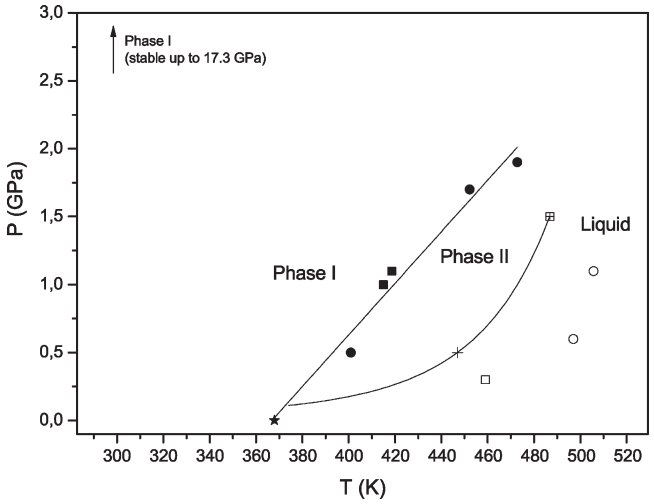

Figure 9. Phase diagram of L-lactide in the investigated pressure and temperature ranges. Circles and squares represent IR and Raman data, respectively. The solid star indicates the melting at ambient pressure. The solid markers indicate the crystal phase transition between phase I and phase II, whereas the empty markers indicate the instability region of L-lactide. The cross symbol indicates the melting in absence of reactivity and the crossed empty square symbol indicates the simultaneous melting and reaction. The solid lines represent a guide for the eye.

On the contrary, the spectra recorded during isobaric heating experiments at higher pressures clearly indicated the occurrence of a phase transition in the L-lactide crystal before the melting. In particular, the complete collapse of the band splitting of the internal vibrational modes (Figures 3 and 7) suggests a transformation to a crystal phase with only one molecule per unit cell. The mid-infrared spectrum in this high-pressure and high-temperature phase was indistinguishable from the spectrum of the liquid. Nevertheless, the Raman spectra collected in the same pressure and temperature conditions, showing the presence of intense bands in the lattice phonon region, allowed to exclude the possibility of melting (Figure 7). This high-pressure and high-temperature phase extends between the ambient pressure crystal phase and the liquid, its stability region becoming larger as the pressure and temperature increase. We will refer to this phase as phase II. As shown in Figure 4, phase II could be recovered at ambient conditions by cooling and decompressing the sample before the occurrence of the reaction. If phase I of L-lactide is the thermodynamically stable phase at ambient conditions, such behavior can be explained by invoking a kinetic metastability of phase II.

The transition to the liquid phase was revealed at higher temperature in the Raman spectra by the disappearance of the sharp lattice phonon bands and by the appearance in the same region of a broad band characteristic of liquid systems. Further information supporting the identification of the melting was the visual observation of the displacement of the ruby chip at the same temperature at which the above-mentioned issues were observed. The data about the I−II phase transition, the melting, and the onset of the reaction are reported in Figure 9, where a phase diagram for L-lactide, entirely traced on the basis of the experimental data from this work, is shown.

Reaction Product. The reaction evolution could be followed at constant thermodynamic conditions by means of the FTIR spectra. Despite the saturation of most of the strong absorptions, both of L-lactide and of the reaction product, it was possible to select some spectral windows where the disappearance of the L-lactide bands and the appearance of the product bands could be detected and followed throughout the whole reactive process (Figure 5). In the spectral range between 600 and 1000 cm^{-1}, the reactant and product bands did not overlap and their absorptions were in scale throughout the whole process.

L-Lactide has absorptions at 605, 773, 793, and 823 cm^{-1} (all of them ring deformations) and 653 cm^{-1} (ring breathing),[33] whereas PLLA has absorptions at 696 and 712 cm^{-1} (γ(C═O), bending), 737 and 756 cm^{-1} (δ(C═O), bending), 872 cm^{-1} (ν(C−COO), stretching), and 922 and 957 cm^{-1} ($r(CH_3)$ + ν(CC)).[34,35] Another frequency region where PLLA shows a strong absorption, not overlapped with any L-lactide band, ranges between 1170 and 1240 cm^{-1}, but in this case the absorption was very strong and the saturation occurred since the early stages of the reaction. In Figure 10 we report the ambient conditions FTIR spectra of L-lactide (trace a), of three crystalline catalyst synthesized PLLAs (traces b, c, d), of an amorphous catalyst synthesized PLDA made from the racemic mixture (trace e), and of the recovered products from this study (traces f, g, h, i). The spectra of the recovered products from the high-pressure and high-temperature experiments agree with that of PLA, even though all the absorption bands appear broader and less structured, especially in the low-frequency region. From Figure 10 the almost complete conversion of L-lactide to PLA is also evident. Only traces of the most intense L-lactide bands can be seen at 650 and 935 cm^{-1}.

The Raman spectra show that the reaction occurs in the liquid phase. The spectral evidence identifying the reaction is the

dx.doi.org/10.1021/jp1110136 |J. Phys. Chem. B 2011, 115, 2173–2184

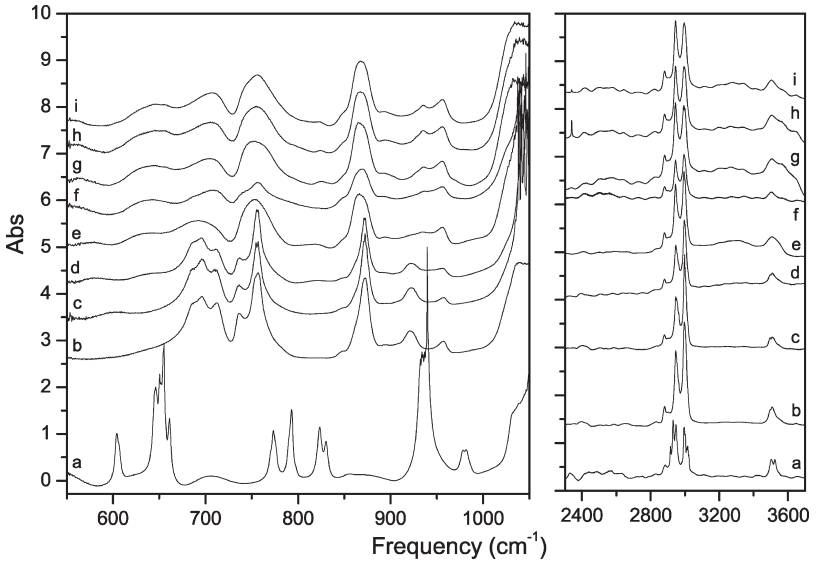

Figure 10. Selected infrared regions showing a comparison among the ambient conditions FTIR spectra of L-lactide (trace a), four catalyst synthesized PLAs (traces b, c, d, e) and the recovered products form the high-pressure reactions (traces f, g, h, i). The details of the labels are (a) L-lactide, (b) catalyst-synthesized purified and recrystallized PLLA after an annealing at 125 °C for 10 days, (c) "rough" catalyst-synthesized PLLA without purification and recrystallization, (d) catalyst-synthesized purified and recrystallized PLLA, (e) catalyst-synthesized purified and recrystallized PLDA, (f) recovered product from the reaction at 0.3 GPa and 459 K (Raman experiment), (g) recovered product from the reaction at 1.1 GPa and 509 K (FTIR experiment), (h) recovered product from the reaction at 1.5 GPa and 487 K (Raman experiment), and (i) recovered product from the reaction at 0.6 GPa and 498 K (FTIR experiment).

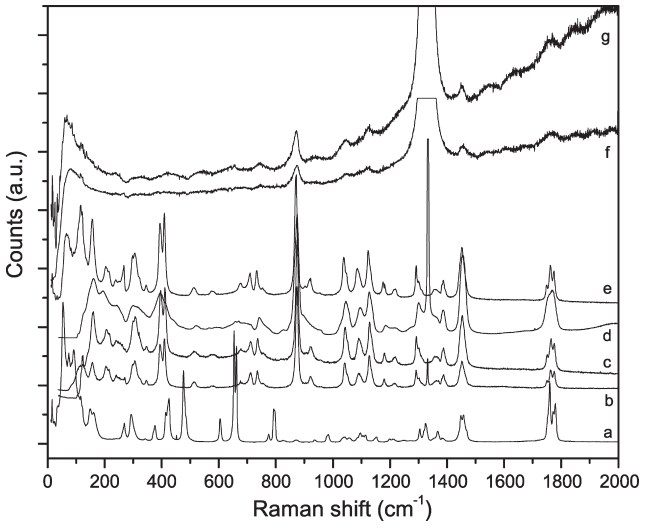

Figure 11. Comparison among the Raman spectra of (a) L-lactide used for the reaction (ambient conditions), (b) "rough" catalyst-synthesized PLLA without purification and recrystallization (ambient conditions), (c) catalyst-synthesized purified and recrystallized PLLA (ambient conditions), (d) catalyst-synthesized purified and recrystallized PLDA (ambient conditions), (e) catalyst-synthesized purified and recrystallized PLLA after an annealing at 125 °C for 10 days, (f) reaction product from the Raman experiment at 1.5 GPa and 487 K (recorded at 1.0 GPa and 499 K), and (g) reaction product from the Raman experiment at 0.3 GPa and 459 K (recorded at 0 GPa and 459 K). The intense band at 1330 cm^{-1} in the spectra b, d, f, and g is the Raman signal of the diamond anvils.

disappearance of the internal bands of L-lactide and the appearance of a new band at 870 cm^{-1} (Figure 7). This band, assigned to a ν(C−COO) vibrational mode, is the most intense in all the PLAs reported in the literature, whatever their stereochemistry.[34,35] Another band at 1454 cm^{-1} ($\delta_{as}(CH_3)$) common to all the PLAs, is also present in our Raman spectra, as well as a broad and weak band at about 1760 cm^{-1} in the carbonyl stretching region (Figure 11). Finally, two other Raman bands peaked at 1045 and 1124 cm^{-1} could be assigned to PLA and in particular to the ν(C−CH_3) stretching and $r(CH_3)$ antisymmetric rocking, respectively.[34,35]

DISCUSSION

The purpose of this study was the investigation of the high-pressure reactivity of L-lactide, aimed at the synthesis without catalysts of PLLA. PLLA can be produced in a large variety of states, from totally amorphous up to 40% crystalline.[8] Semicrystalline PLLA can be obtained when using more than 93% of L-lactic acid, whereas amorphous PLLA is obtained from an amount of L-lactic acid between 50 and 93%. The presence of D-lactide and meso forms produces crystalline imperfections and reduces the crystallinity percentage. An important role in the obtainment of crystalline materials is played by the application of suitable annealing treatments. The extension of the amorphous fraction, the crystallinity percentage of the polymeric material, and the morphology and chain orientation are of fundamental importance for practical applications because they determine the thermal and mechanical properties of the material.

Depending on the processing conditions, PLLA can crystallize in three different forms: α, β, and γ.[8,36,37] The α form is the most common when PLLA is obtained under normal conditions from the solution or the melt. The space group for the α-form is orthorhombic ($P2_12_12_1$, a = 10.66 Å, b = 6.16 Å, c = 28.88 Å) and the unit cell contains two antiparallel chains with distorted helical conformation. The β form can be prepared at very high draw ratio and high temperature. The chain conformation is a left handed 3-fold helix. The β-form has an orthorhombic unit cell containing a 3_1 polymeric helix (a = 10.31 Å, b = 18.21 Å, c = 9.0 Å). The structure of this form

is still debated and the chain packing of the β form has been recently considered a frustrated structure containing three 3-fold helices per unit cell ($P3_2$, $a = b = 10.52$ Å, $c = 8.8$ Å).[38] The α-structure is more stable than the β-structure. The γ-structure, obtained by epitaxial growth, has been suggested to contain two antiparallel helices arranged in an orthorhombic unit cell ($a = 9.95$ Å, $b = 6.25$ Å, $c = 8.8$ Å) and to assume the 3-fold helix of polylactides.[39] Depending on the crystallinity, the molecular weight, and the morphology, the glass transition temperature T_g of PLLA ranges between 326 and 337 K and the melting temperature T_m between 418 and 459 K.[40] Our reactions were performed at temperature between 450 and 509 K. Even though no literature data about the behavior of T_g and T_m at high pressure are available, an increase in these values is likely to be expected, due to the increased density at high pressure. For this reason, it was not possible to state whether the reaction product was obtained in the liquid or in the solid phase during the formation.

The comparison of the recovered products with several catalyst synthesized PLAs indicates the obtainment of an amorphous PLA (Figure 10). Several spectral indications support this conclusion. First, the crystalline catalyst synthesized PLLAs (Figure 10, traces b, c, d) show two characteristic bands at 922 and 957 cm^{-1}, whereas our reaction products (Figure 10, traces f, g, h, i) show only one band at 957 cm^{-1}. The weak band at 935 cm^{-1} has to be assigned to traces of unreacted L-lactide. Kister et al.[34,35] have studied the effect of morphology, conformation, and configuration on the vibrational spectrum of various PLAs using infrared and Raman spectroscopy. In particular, they have compared one semicrystalline PLLA with an amorphous one and found that the semicrystalline PLLA shows a typical Raman band at 923 cm^{-1} identified as a characteristic helical backbone vibration mixed with CH_3 rocking modes. They have reported a corresponding infrared band for this vibration at 925 cm^{-1}. Other papers support this assignment indicating an infrared band at 923 cm^{-1}, which is absent in the completely amorphous PLA, as a typical feature of the α crystalline polymer involving the C−COO stretching, the O−CH stretching and the CH_3 rocking.[41−43] The band at 957 cm^{-1} is present in any kind of PLA, whatever the stereochemistry, morphology, and crystallinity. The intensity of this band is reported to decrease during thermal and mechanical treatments of the sample for increasing the crystallinity, while the crystallinity marker absorption for the α-phase at 923 cm^{-1} grows in intensity.[41,42,44] A quantitative determination of the crystallinity percentage is possible from the loss of absorption of the band at 957 cm^{-1}.[41] The band shape of the infrared absorption at 870 cm^{-1} is also a crystallinity indicator. This band is present in any kind of PLA, but it is sharper in the crystalline ones (Figure 10, traces b, c, d) and broader in the amorphous ones (Figure 10, trace e). Our recovered products (Figure 10, traces f, g, h, i) show a broad signal similar to that of an amorphous polymer. Furthermore, in the crystalline PLLAs two distinct components can be distinguished at 736 and 756 cm^{-1}, whereas our recovered products present a broad signal in this region. Only in the sample recovered from the Raman experiment at 0.3 GPa and 459 K the two components can be identified. Finally, the crystalline PLLAs show three overlapped bands at 685, 696, and 712 cm^{-1}, whereas the recovered products from this study only show a broad unresolved absorption. The β-form of crystalline PLA has a characteristic infrared band at 912 cm^{-1},[45] which is not observed in any of our recovered products, and can thus be confidently excluded. Therefore, the infrared spectra of our recovered products show striking similarities with that reported in Figure 10e, corresponding to PLDA. PLDA was synthesized from a racemic mixture of L,L and D,D lactides. The presence of different stereocenters ensured the obtainment of an amorphous material. As the obtainment of a completely amorphous PLLA is not easy and vibrational spectroscopy is unable to discriminate between L and D stereocenters, we used PLDA as a reference for an amorphous PLA.

Despite the great utility of the Raman spectra in providing information on the morphology and crystallinity of PLLA, our Raman experiments are useless for characterizing the reaction product, due to the unresolved structure of the Raman spectra collected at high temperature (Figure 11). Moreover, the measurement of the Raman spectra during the decompression and cooling stages was also prevented by the damaging of the sample with the laser light (Figure 8).

Two aspects likely contributed to the formation of an amorphous PLA. The first one is related to the cooling rate of the sample after the end of the reaction, which was not controlled, so that the formation of an amorphous phase might have occurred due to a too high cooling rate. The second one is related to the risk of racemization of L-lactide at high temperature.[8,46] At ambient pressure the suitable reaction temperature of L-lactide for maintaining the appropriate viscosity should be around 463−473 K, but in these conditions the racemization is not a minor side reaction. For this reason, the employed temperature on a laboratory scale is lowered to the 393−410 K interval, which provides a good compromise between efficiency and minimization of the racemization. In our case, the reaction temperatures ranged between 459 and 509 K, but we cannot predict the effect of the pressure on the racemization process. Moreover, the D,D- and L,L-lactide are not distinguishable on the basis of their vibrational spectra. For this reason, we preferred to label the reaction product as PLA and not as PLLA. Nevertheless, if the stereochemistry is preserved, the obtainment of an amorphous polymer is not a drawback: PLLA obtained by catalytic methods shows a high crystalline character only after thermal curing.

Our infrared spectra revealed the formation of CO_2 and the appearance of a weak broad absorption in the region between 2800 and 3600 cm^{-1}, typically associated with O−H stretching vibrations involved in hydrogen bond interactions. The appearance of these two features coincided with a slight decrease in the intensity of the product bands in the 600−1000 cm^{-1} region (Figure 5). For this reason, we associated them with a decomposition of PLA rather than with a secondary reaction involving the residual L-lactide. The decomposition process occurred with a certain delay with respect to the polymerization reaction. In the FTIR experiment at 0.6 GPa and 498 K, we monitored the growth of the CO_2 band since its early appearance to immediately detect any sudden increase in the slope of the growth curve in order to stop the decomposition process in its early stages and preserve the synthesized polymer. Nevertheless, no significant differences could be observed in the spectrum of the recovered product obtained according to this procedure with respect to the others (Figure 10). The thermal decomposition (pyrolysis) of PLA, with the formation of volatile products, is reported to occur at ∼300 °C. The volatile products consist of cyclic oligomers, lactide, acetaldehyde, carbon monoxide, and carbon dioxide.[47] In particular, acetaldehyde and carbon dioxide continuously form during the heating. A combination of thermogravimetric analysis (TGA) and FTIR spectroscopy has been used to study the decomposition of PLA at ambient pressure in nitrogen and oxygen atmosphere.[48] In a nitrogen atmosphere the degradation

takes place beyond 300 °C. At the beginning, the decomposition products are mainly acetaldehyde, carbon monoxide, carbon dioxide, water, and methane, whereas at higher temperature also the formation of L-lactide is observed. A more detailed analysis using thermogravimetric analysis and FTIR correlation spectroscopy indicates also the formation of acetic anhydride and acetic acid.[48] In oxygen atmosphere, PLA first oxidizes to CO, CO_2, water, and short-chain acids; then also in this case L-lactide forms at higher temperature.[48] Other studies confirm these reports.[49,50] Our experiments do not contain either nitrogen or oxygen because the cell was sealed under vacuum. The absence of oxidants makes our results reasonably comparable to the literature data referring to an inert nitrogen atmosphere. The appearance of a broad absorption band due to O−H groups could be consistent with the formation of water and acetic acid. Nevertheless, acetic acid exhibits an infrared band of medium intensity at 620 cm^{-1}, which is not present in our spectra and can thus be confidently excluded. Acetic anhydride can also be ruled out because it exhibits two strong bands at 897 and 997 cm^{-1} and none of them is observed in our spectra. The formation of acetaldehyde, indicated as one of the main decomposition products,[48] cannot be confirmed nor excluded, because its absorption bands overlap with the out of scale bands of PLA. Besides the formation of H_2O, the broad absorption in the O−H stretching region could indicate the occurrence of enolization processes of the PLA chains during the decomposition reaction. This intramolecular reaction mechanism, leading to the formation of PLA oligomers, would take into account the racemization of the PLA stereocenters and the cleavage of the PLA chains, supporting the formation of an amorphous PLA.[50,51] The activation of this decomposition channel, which opens after a time delay, may be related to the modification of the reaction environment as the reaction proceeds and in particular to the lack of L-lactide molecules, so that intramolecular processes, such as the decomposition, may occur instead of the propagation of the polymerization.

Finally, a few considerations can be made about the reaction mechanism. The duration of the reaction extended from a few hours in the case of the Raman experiments (0.3 GPa-459 K and 1.5 GPa-487 K) to 42 h in the case of the FTIR experiment at 1.1 GPa-509 K, and up to 835 h in the case of the FTIR experiment at 0.6 GPa-498 K. This experimental evidence indicates that the laser wavelength (647.1 nm) employed for the Raman experiments somehow increased the reaction rate. According to the UV−vis absorption spectrum of L-lactide, which we measured at ambient conditions identifying an absorption onset at 270 nm, and to computational results reporting the first singlet excited state of L-lactide at 228.91 nm,[52] an unlikely three-photon absorption process would be necessary for its excitation. On the other hand, PLA starts to absorb at ∼300 nm,[8] thus making possible a two-photon absorption at the wavelength used for the Raman experiments, even taking into account a likely red shift of the electronic transition at high pressure. As reported in several cases, the formation of excited species can generate active species and facilitate the propagation of the reaction through the branching of the polymeric chains.[13]

The very different duration of the reaction in the two FTIR experiments cannot be ascribed either to the laser irradiation for the measurement of pressure (less than 1 mW at 532.8 nm was always used for this purpose) or to the temperature, which was comparable in the two cases. Therefore, the different reaction pressure must be considered responsible for the different duration of the reaction in the two experiments. The reaction was indeed accelerated at least by a factor 20 for an increase of pressure from 0.6 GPa (498 K) to 1.1 GPa (509 K), thus indicating a rate-determining step characterized by a volume reduction (negative activation volume $\Delta V^{\ddagger}$). Considering a simplified reaction scheme for the chain growth, in which the diffusion of two L-lactide molecules is followed by the opening of the L-lactide ring, we may imagine a negative $\Delta V^{\ddagger}$ for the molecular diffusion step and a positive $\Delta V^{\ddagger}$ for the ring-opening one and identify the first one as the rate-limiting step. Such a mechanism is also supported by the coincidence of the reaction with the melting at high pressure (Raman experiment at 1.5 GPa-487 K), whereas at low pressure (Raman experiment at 0.3 GPa-459 K) we first observed the melting and then the reaction for a higher temperature, as clearly shown in Figure 9. The occurrence of the reaction only in the liquid phase indeed supports the key role played in the reaction mechanism by the diffusion step and therefore by the molecular mobility. This was also evidenced by the stability of L-lactide in the crystalline phase I at room temperature up to 17.3 GPa.

CONCLUSIONS

In this study we traced a phase diagram of L-lactide on the basis of FTIR and Raman spectroscopy. The room temperature crystal phase (phase I) of L-lactide is stable up to 17.3 GPa at 300 K. Another crystal phase (phase II) exists at high pressure between the phase I and the liquid. Increasing the temperature from phase II, a reaction was observed in the compressed liquid, where L-lactide was found to polymerize in the total absence of solvents, catalysts, and radical initiators. The reaction was studied in different pressure and temperature conditions by using FTIR and Raman spectroscopy. In all the experiments, the almost complete transformation of L-lactide to PLA was observed. The only observed difference was related to the faster reaction rate in the Raman experiments with respect to the FTIR ones in comparable thermodynamic conditions. The role of the laser light in the process is still unclear and requires further investigations because it may turn out to be a valuable method for speeding up the reaction without affecting the reaction product. Within the investigated experimental conditions, the reaction only occurred in the liquid, suggesting the presence of some steric hindrances in the crystal which prevent the effective intermolecular approach. The FTIR experiments performed at different pressures in the absence of irradiation showed that pressure markedly increases the reaction rate, indicating that the rate-determining step of the reaction mechanism is characterized by a negative activation volume. This conclusion is also supported by the Raman experiments. The analysis of the spectra indicated the obtainment of a completely amorphous PLA, as demonstrated by the absence of the band at 923 cm^{-1} typical of the α-crystalline structure of PLLA. The amorphous character of the material was likely due to conformational disorder of the PLA chains; however, it was not possible to exclude the occurrence of racemization at high temperature. The presence of different stereocenters could in fact be responsible for an imperfect packing of the polymer chains and hence for the formation of an amorphous material. A decomposition reaction took place after a certain time delay since the beginning of the reaction, leading to the formation of hydroxyl groups and to the elimination of CO_2. The extension of this decomposition process could be limited by monitoring the growth of the CO_2 antisymmetric

stretching absorption, which is a very sensitive marker. The reaction conditions reported in this study are not far from the limits of the current industrial technology, especially if pressure and temperature are applied in combination with laser irradiation. The application of thermodynamic conditions accessible to the current industrial technologies and the absence of solvents, catalysts, and radical initiators make this process appealing for possible scaling of the experimental system to large volume apparatuses, opening new possibilities for the synthesis of amorphous PLA according to green chemistry requirements.

AUTHOR INFORMATION

Corresponding Author

*E-mail: ceppa@lens.unifi.it.

ACKNOWLEDGMENT

Supported by the European Union FP7 G.A. No 228334-LASERLAB EUROPE, the Regione Toscana ("Competitività regionale e occupazione" 2007-2013, project TeCon@BC, POR-FESR 2007-2013) and MIUR (PRIN 2008 project 200898KCKY, "Inorganic nanohybrids based on bio-polyesters from renewable resource").

REFERENCES

(1) *Handbook of Biodegradable Polymers*; Bastioli, C., Ed.; Rapra Technology Ltd.: Shrewsbury, UK, 2005; ISBN: 1-85957-389-4. Gross, R. A.; Kalra, B. *Science* **2002**, *803*, 297. Garlotta, D. *J. Polym. Environ.* **2002**, *63*, 9. Mohanty, A. K.; Misra, M.; Drzal, L. T. *J. Polym. Environ.* **2002**, *10*, 19.

(2) Drumright, R. E.; Gruber, P. R.; Henton, D. E. *Adv. Mater.* **2000**, *12*, 1841.

(3) Lunt, J. *Polym. Degrad. Stab.* **1998**, *59*, 145.

(4) Zhang, Z. Y.; Jin, B.; Kelly, J. M. *World J. Microbiol. Biotechnol.* **2007**, *23*, 229. Rojan, P. J.; Nampoothiri, K. M.; Pandey, A. *Appl. Microbiol. Biotechnol.* **2007**, *74*, 524. Onda, A.; Ochi, T.; Kajiyoshi, K.; Yanagisawa, K. *Catal. Commun.* **2008**, *9*, 1050. Tari, C.; Ustok, F. I.; Harsa, S. *Int. Dairy J.* **2009**, *19*, 236. Mondragon-Parada, M. E.; Najera-Martinez, M.; Juarez-Ramirez, C.; Galindez-Mayer, J.; Ruiz-Ordaz, N.; Cristiani-Urbina, E. *Appl. Biochem. Biotechnol.* **2006**, *134*, 223.

(5) Datta, R.; Tsai, S.; Bonsignore, P.; Moon, S.; Frank, J. *FEMS Microbiol. Rev.* **1995**, *16*, 221.

(6) Sakai, K.; Taniguchi, M.; Miura, S.; Ohara, H.; Matsumoto, T.; Shirai, Y. *J. Ind. Ecol.* **2004**, *7*, 63.

(7) Li, D.; Frey, M. W.; Vynias, D.; Baeumner, A. J. *Polymer* **2007**, *48*, 6340. Albertsson, A. C.; Varma, I. K. *Biomacromolecules.* **2003**, *4*, 1466.

(8) Auras, R.; Harte, B.; Selke, S. *Macromol. Biosci.* **2004**, *4*, 835.

(9) Pang, K; Kotek, R.; Tonelli, A. *Prog. Polym. Sci.* **2006**, *31*, 1009. Wu, J.; Yu, T. L.; Chen, C.-T.; Lin, C.-C. *Coord. Chem. Rev.* **2006**, *250*, 602. Coulembier, O.; Degee, P.; Hedrick, J. L.; Duboi, P. *Prog. Polym. Sci.* **2006**, *31*, 723. Dechy-Cabaret, O.; Martin-Vaca, B.; Bourissou, D. *Chem. Rev.* **2004**, *104*, 6147. Kowalski, A.; Duda, A.; Penczek, S. *Macromol. Rapid Commun.* **1998**, *19*, 567.

(10) Du, Y. J.; Lemstra, P. J.; Nijenhuis, A. J.; Van Aert, H. A. M.; Bastiaansen, C. *Macromolecules* **1995**, *28*, 2124. Kricheldorf, H. R.; Kreiser-Saunders, I.; Boettcher, C. *Polymer* **1995**, *36*, 1253. Kurcok, P.; Penczek, J.; Franek, J.; Kedlinski, Z. *Macromolecules* **1992**, *25*, 2285. Kricheldorf, H. R.; Kreiser, I. *Makromol. Chem.* **1987**, *188*, 1861.

(11) Frediani, M.; Semeril, D.; Mariotti, A.; Rosi, L.; Frediani, P.; Rosi, L.; Matt, D.; Toupet, L. *Macromol. Rapid Commun.* **2008**, *29*, 1554. Umare, P. S.; Tembe, G. L.; Rao, K. V.; Satpathy, U. S.; Trivedi, B. *J. Mol. Catal. A: Chem.* **2007**, *268*, 235. Lee, J.; Kim, Y.; Do, Y. *Inorg. Chem.* **2007**, *46*, 7701. Ejfler, J.; Kobyka, M.; Jerzykiewicz, L. B.; Sobota, P. *J. Mol. Catal. A: Chem.* **2006**, *257*, 105. Dove, A. P.; Pratt, R. C.; Lohmeijer, B. G. G.; Culkin, D. A.; Hagberg, E. C.; Nyce, G. W.; Waymouth, R. M.; Hedrick, J. L. *Polymer* **2006**, *47*, 4018. Ovitt, T. M.; Coates, G. W. *J. Am. Chem. Soc.* **2002**, *124*, 1316. Takashima, Y.; Nakayama, Y.; Watanabe, K.; Itono, T.; Ueyama, N.; Nakamura, A.; Yasuda, H.; Harada, A. *Macromolecules* **2002**, *35*, 7538.

(12) *Handbook of polymer synthesis*; Kricheldorf, H. R., Nuyken, O., Swift, G., Eds.; Marcel Dekker: New York, 2005.

(13) Schettino, V.; Bini, R.; Ceppatelli, M.; Ciabini, L. Citroni, M. Chemical reactions at very high pressure. In *Advances in Chemical Physics*; Rice, S. A., Ed.; Wiley-Interscience: New York, 2005; Vol. 131, pp 105−242.

(14) Lundegaard, L. F.; G. Weck, G.; McMahon, M. I.; Desgreniers, S.; Loubeyre, P. *Nature* **2006**, *443*, 201.

(15) Eremets, M. I.; Hemley, R. J.; Mao, H. K.; Gregoryanz, E. *Nature* **2001**, *411*, 170.

(16) Eremets, M. I.; Gavriliuk, A. G.; Trojan, I. A.; Dzivenko, D. A.; Boehler, R. *Nat. Mater.* **2004**, *3*, 558.

(17) Santoro, M.; Gorelli, F. A.; Bini, R.; Ruocco, G.; Scandolo, S.; Crichton, W. A. *Nature* **2006**, *441*, 857.

(18) Aoki, K.; Kakudate, K.; Yoshida, M.; S. Usuba, S.; Fujiwara, S. *J. Chem. Phys.* **1989**, *91*, 778.

(19) Yoo, C. S.; Nicol, M. *J. Phys. Chem.* **1986**, *90*, 6726; **1986**, *90*, 6732.

(20) Ceppatelli, M.; Santoro, M.; Bini, R.; Schettino, V. *J. Chem. Phys.* **2000**, *113*, 5991.

(21) Citroni, M.; Ceppatelli, M.; Bini, R.; Schettino, V. *J. Chem. Phys.* **2003**, *118*, 1815.

(22) Chelazzi, D.; Ceppatelli, M.; Santoro, M.; Bini, R.; Schettino, V. *J. Phys. Chem. B* **2005**, *109*, 21658.

(23) Ciabini, L.; Santoro, M.; Gorelli, F. A.; Bini, R.; Schettino, V.; Raugei, S. *Nat. Mater.* **2007**, *6*, 39.

(24) Lipp, M. J.; Evans, W. J.; Baer, B. J.; Yoo, C. S. *Nat. Mater.* **2005**, *4*, 211.

(25) Ceppatelli, M.; Bini, R.; Schettino, V. *Proc. Natl. Acad. Sci. U.S. A.* **2009**, *106*, 11454.

(26) Bini, R. *Acc. Chem. Res.* **2004**, *37*, 95.

(27) Citroni, M.; Ceppatelli, M.; Bini, R.; Schettino, V. *Science* **2002**, *295*, 2058.

(28) Chelazzi, D.; Ceppatelli, M.; Santoro, M.; Bini, R.; Schettino, V. *Nat. Mater.* **2004**, *3*, 470.

(29) Mao, H. K.; Bell, P. M.; Shaner, J. V.; Steinberg, D. J. *J. Appl. Phys.* **1978**, *49*, 3276.

(30) Bini, R.; Ballerini, R.; Pratesi, G.; Jodl, H. J. *Rev. Sci. Instrum.* **1997**, *68*, 3154.

(31) Gorelli, F.; Santoro, M.; Ulivi, L.; Bini, R. *Phys. Rev. Lett.* **1999**, *83*, 4093.

(32) Van Hummel, G. J.; Harekma, S.; Kohn, F. E.; Feijen, J. *Acta Crystallogr.* **1982**, *B38*, 1679.

(33) Tam, C. N.; Bour, P.; Keiderling, T. A. *J. Am. Chem. Soc.* **1996**, *118*, 10285.

(34) Kister, G.; Cassanas, G.; Vert, M. *Polymer* **1998**, *39*, 267.

(35) Kister, G.; Cassanas, G.; Vert, M.; Pauvert, B.; Térol, A. *J. Raman Spectrosc.* **1995**, *26*, 307.

(36) Krikorian, V.; Pochan, D. *Macromolecules* **2005**, *38*, 6520.

(37) Sasaki, S.; Asakura, T. *Macromolecules* **2003**, *36*, 8385.

(38) Cartier, J.; Ikada, Y.; Tsuji, H.; Cartier, L.; Okihara, T.; Lotz, B. *Polymer* **2000**, *41*, 8921.

(39) Cartier, L.; Okiharaa, T.; Ikadab, Y.; Tsujic, H.; Puiggalia, J.; Lotza, B. *Polymer* **2000**, *41*, 8909.

(40) Gupta, B.; Revagade, N.; Hilborn, J. *Prog. Polym. Sci.* **2007**, *32*, 455.

(41) Meaurio, E.; López-Rodriguez, N.; Sarasua, J. R. *Macromolecules* **2006**, *39*, 9291.

(42) Zhang, J.; Tsuji, H.; Noda, I.; Ozaki, Y. *J. Phys. Chem. B* **2004**, *108*, 11514.

(43) Kang, S.; Hsu, S. H.; Stidham, H.; Smith, P. B.; Leugers, A. M.; Yang, X. *Maromolecules* **2001**, *34*, 4542.

(44) Lee, J. K.; Lee, K. H.; Jin, B. S. *Eur. Polym. J.* **2004**, *37*, 907.
(45) Sawai, D.; Takahashi, K.; A. Sasashige, A.; Kanamoto, T. *Macromolecules* **2003**, *36*, 3061–3605.
(46) Tsukegi, T.; Motoyama, T.; Shirai, Y.; Nishida, H.; Endo, T. *Polym. Degrad. Stab.* **2007**, *92*, 552.
(47) Zou, H.; Yi, C.; Wang, L.; H. Lou, H.; Xu, W. *J. Therm. Anal. Calorim.* **2009**, *97*, 929.
(48) Vogel, C.; Siesler, H. W. *Macromol. Symp.* **2008**, *265*, 183.
(49) McNeill, I. C.; Leiper, H. A. *Polym. Degrad. Stab.* **1985**, *11*, 309.
(50) Kopinke, F. D.; Remmler, M.; Mackenzie, K.; Möder, M.; Wachsen, O. *Polym. Degrad. Stab.* **1996**, *53*, 329.
(51) Kopinke, F. D.; Mackenzie, K. *J. Anal. Appl. Pyrol.* **1997**, *40−41*, 43.
(52) Wu, W.; Li, W.; Wang, L.; Zhang, P.; Zhang, J. *THEOCHEM* **2007**, *816*, 13.